

# GLP-1 stimulates glucose-derived de novo fatty acid synthesis and chain elongation during cell differentiation and insulin release

Angela Bulotta,\* Riccardo Perfetti,\* Hongxiang Hui,\* and László G. Boros<sup>1,†</sup>

Division of Endocrinology,\* Cedars-Sinai Medical Center 8723 Alden Drive, SSB 290 Los Angeles, CA 90048; and Harbor-UCLA Research and Education Institute,<sup>†</sup> UCLA School of Medicine, 1124 West Carson Street, RB1, Torrance, CA 90502

**Abstract** Glucagon-like peptide-1 (GLP-1, 7-36) is capable of restoring normal glucose tolerance in aging, glucose-intolerant Wistar rats and is a potent causal factor in differentiation of human islet duodenal homeobox-1-expressing cells into insulin-releasing  $\beta$  cells. Here we report stable isotope-based dynamic metabolic profiles of rat pancreatic epithelial (ARIP) and human ductal tumor (PANC-1) cells responding to 10 nM GLP-1 treatment in 48 h cultures. Macromolecule synthesis patterns and substrate flow measurements using gas chromatography/mass spectrometry (MS) and the stable [1,2-<sup>13</sup>C<sub>2</sub>]glucose isotope as the tracer showed that GLP-1 induced a significant 20% and 60% increase in de novo fatty acid palmitate synthesis in ARIP and PANC-1 cells, respectively, and it also induced a significant increase in palmitate chain elongation into stearate utilizing glucose as the primary substrate. Distribution of <sup>13</sup>C in other metabolites indicated no changes in the rates of nucleic acid ribose synthesis, glutamate oxidation, or lactate production. Tandem high-performance liquid chromatography-ion trap MS analysis of the culture media demonstrated mass insulin secretion by GLP-1-treated tumor cells. **Metabolic profile changes in response to GLP-1-induced cell differentiation include selective increases in de novo fatty acid synthesis from glucose and consequent chain elongation, allowing increased membrane formation and greater insulin availability and release.**—Bulotta, A., R. Perfetti, H. Hui, L. G. Boros. GLP-1 stimulates glucose-derived de novo fatty acid synthesis and chain elongation during cell differentiation and insulin release. *J. Lipid Res.* 2003. 44: 1559–1565.

**Supplementary key words** glucagon-like peptide-1 • stable isotope-based dynamic metabolic profiling • pentose cycle • insulin production • stable isotope trace • mass spectrometry • SIDMAP

Glucagon-like peptide-1 (GLP-1; 7-36) of the intestine enhances insulin secretion from pancreatic  $\beta$  cells in response to food intake and restores normal glucose tolerance in glucose-intolerant aging Wistar rats (1). Expression of insulin mRNA and high insulin contents were described

after transfection of insulinoma cells with the GLP-1 receptor in epithelial cells of the pancreas (2). Additionally, both rat and human cells readily differentiate into insulin-secreting cells in response to GLP-1 treatment (3, 4). Cell differentiation and insulin release by pancreatic cells in response to GLP-1 require the presence of functioning specific receptors and the presence of the islet duodenal homeobox-1 (PDX-1) transcript protein, which translocates to the nucleus (5). This process is triggered by a ligand-induced activation of adenylyl cyclase that increases intracellular cAMP levels, which, in turn, activate protein kinase A during epithelial cell differentiation (6, 7).

Stable isotope-based dynamic metabolic profiling (SIDMAP) technology helps detail mechanisms of hormone actions by revealing genotype-phenotype-metabolome interactions and by tracking metabolic pathway substrate flow changes (Fig. 1) (8, 9). Fatty acid metabolism appears to be a critical factor in cell differentiation and in mediating the anti-tumor activities of newly characterized potent kinase targeting treatment modalities (10–13). In the present study, we have investigated the metabolic substrate flow regulating effects of GLP-1 in two epithelial tumor cell lines, which both differentiate into insulin-secreting  $\beta$ -like cells in culture. This paper demonstrates that cell differentiation and regulation of insulin release after GLP-1 treatment are accompanied by important metabolic adaptive changes that primarily affect the contribution of glucose to de novo fatty acid synthesis and chain elongation of the saturated long-chain species primarily utilized for triglyceride and membrane synthesis.

## MATERIALS AND METHODS

### Cell line and culture

Rat pancreatic epithelial (ARIP) pancreatic epithelial carcinoma cells (American Type Culture Collection, Manassas, VA)

Manuscript received 26 February 2003 and in revised form 18 May 2003.

Published, JLR Papers in Press, June 1, 2003.  
DOI 10.1194/jlr.M300093JLR200

<sup>1</sup> To whom correspondence should be addressed.  
e-mail: boros@gcrc.rei.edu

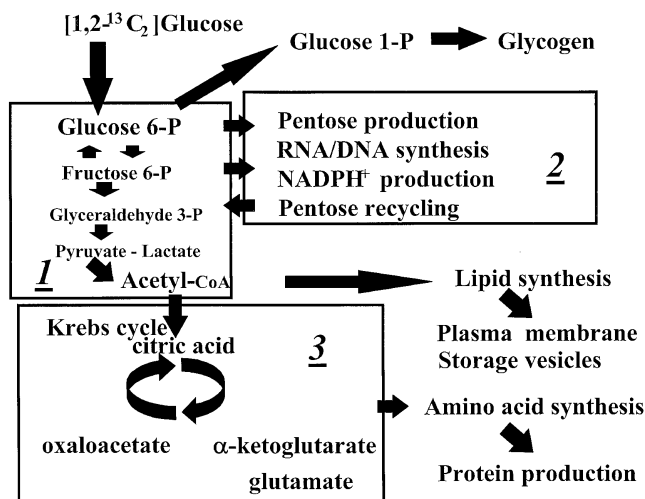


**Fig. 1.** Metabolic profiling of interconnected metabolic pathways and their dynamic cross-labeling by  $^{13}\text{C}$ -labeled glucose as the precursor. D-[1,2- $^{13}\text{C}_2$ ]-glucose readily labels major metabolite pools either as a direct substrate or through carbon exchange. The specificity for metabolic pathway substrate flow measurement is provided by the loss and rearrangements of the  $^{13}\text{C}$  label from [1,2- $^{13}\text{C}_2$ ]-glucose in various metabolite, intermediate, and product pools. Box 1 represents glycolysis, box 2 represents the pentose cycle, and box 3 represents the TCA cycle. The metabolic effects of glucagon-like peptide-1 (GLP-1) treatment are demonstrated in this study by determining the destinies of the  $^{13}\text{C}$  tracer throughout metabolism (8, 9) using stable isotope-based dynamic metabolic profiling.

were grown in F12 medium in the presence of 10% FBS at 37°C in a 95% air-5%  $\text{CO}_2$  mixture. Human ductal tumor (PANC-1) cells were purchased from ATCC and transfected with the full-length human PDX-1 gene, as previously described (3). The transfected PANC-1/PDX-1 cells were grown in complete DMEM (10% FBS, 1% penicillin/streptomycin) (T75 flasks). When the cells were 70–80% confluent, the adherent cell layer was washed with serum-free medium followed by a “wash-out” overnight incubation with serum-free DMEM. The cells were then cultured for 48 h with serum-free DMEM without glucose-containing GLP-1 (10 nM, every 8 h) in the presence of 50% [1,2- $^{13}\text{C}_2$ ]-glucose tracer (90 mg/dl) and 50% cold [U- $^{12}\text{C}$ ]-glucose (90 mg/dl). Control flasks were cultured with serum-free DMEM with the glucose tracer without treatment with GLP-1. After 48 h, the media (5 ml) were collected and the cells were harvested by trypsin-EDTA. The media and cell pellets were frozen for subsequent processing. Experiments for each condition were performed in triplicate and repeated once.

Cultures for the study were selected with the same cell number ( $6 \times 10^7$ ), which was achieved using standard cell counting techniques. Media glucose and lactate levels were measured using a Cobas Mira chemistry analyzer (Roche). Glucose oxidation was measured by media  $^{13}\text{C}/^{12}\text{C}$  ratios in released  $\text{CO}_2$  by a Finnegan Delta-S isotope ratio mass spectroscope.  $^{13}\text{CO}_2$  release was used to estimate glucose carbon utilization through oxidation by the cell lines and was expressed as atom percent excess, which is the percent of  $^{13}\text{C}$  produced by the cultured cells above background in calibration standard samples (14).

### Stable isotope based metabolic profiling

The tracer D-[1,2- $^{13}\text{C}_2$ ]-glucose isotope was purchased with >99% purity and 99% isotope enrichment for each position (Isotec, Inc., Miamisburg, OH). For isotope incubation and drug

treatment studies, fibroblasts were seeded in T-75 tissue culture flasks after adjusting the number of cells to the values reported above. During the study, the cultures were supplied with 50% [1,2- $^{13}\text{C}_2$ ]-glucose dissolved in otherwise glucose- and sodium pyruvate-free medium. The rearrangement of glucose  $^{13}\text{C}$  labels in glucose intermediary metabolites and various cellular metabolites revealed by the stable isotope-based metabolic profiling method has previously been described in detail (Fig. 1) (9).

RNA ribose was isolated by acid hydrolysis of cellular RNA after Trizol purification of cell extracts. Ribose was derivatized to its aldonitrile acetate form using hydroxylamine hydrochloride in pyridine and acetic anhydride. We monitored the ion cluster around the  $m/z$  256 [carbons 1–5 of ribose, chemical ionization (CI)],  $m/z$  217 (carbons 3–5 of ribose), and  $m/z$  242 [carbons 1–4 of ribose, electron impact ionization (EI)] in order to determine molar enrichment and positional distribution of  $^{13}\text{C}$  labels in ribose.

DNA deoxyribose was isolated by enzyme digestion and organic extraction by the modified method of Neese et al. (15). In brief, DNA was separated from RNA using the consecutive steps of the RNA isolation process described in the Trizol method. After DNase, phosphodiesterase, and alkaline phosphatase digestions, which yield nucleosides, samples were further hydrolyzed and derivatized in 2% hydroxylamine-pyridine solution (100°C for 1 h). Acetic anhydride was added at room temperature for 1 h to yield the aldonitrile acetate derivative of deoxyribose for analysis with the gas chromatography (GC)/mass spectrometry (MS) instrument. We used a 200 ml methylene chloride and 3 ml water mixture to separate derivatized deoxyribose from salts, phosphate, and inorganic components after the digestion and derivatization processes. We monitored the ion cluster around the  $m/z$  198 (carbons 1–5 of deoxyribose, CI) in order to determine molar enrichment of  $^{13}\text{C}$ -labeled carbons in deoxyribose.

Lactate from the cell culture media (0.2 ml) was extracted by ethyl acetate after acidification with HCL, derivatized to its propylamine-HFB form, and the  $m/z$  328 (carbons 1–3 of lactate, CI) was monitored for the detection of  $m1$  (recycled lactate through the PC) and  $m2$  (lactate produced by the Embden-Meyerhof-Parnas pathway) for the estimation of pentose cycle activity (16).

For glutamate analyses, tissue culture medium was first treated with 6% perchloric acid. Proteins were removed by centrifugation, and the supernatant was neutralized with potassium hydroxide. The neutralized supernatant was passed through a set of Dowex-50 (H+) and Dowex-1 (acetate) columns for the isolation of glutamate and conversion to its trifluoroacetyl butyl ester (TAB) as described elsewhere (17, 18). Under EI conditions, ionization of TAB-glutamate gives rise to two fragments,  $m/z$  198 and  $m/z$  152, corresponding to  $\text{C}_2\text{-C}_5$  and  $\text{C}_2\text{-C}_4$  of glutamate, respectively, which are routinely analyzed during the determination of TCA cycle carbon flow.

Cholesterol and fatty acids were extracted after saponification of the Trizol extract after RNA and DNA separation using 30% KOH and 100% ethanol with petroleum ether. Fatty acids were converted to their methylated derivative using 0.5 N methanolic-HCL. The  $^{13}\text{C}$ -enrichment of acetyl units and the synthesis of the new lipid fraction in response to GLP-1 treatment were determined using the mass isotopomer distribution analysis approach of different isotopomers of palmitate, stearate, and oleate, as reported previously (19).

Insulin from the cell culture media of ARIP cells was isolated using the method described by Khaksa et al. for rat and human blood plasma high-performance liquid chromatography (HPLC) analyses (20). In brief, 1 ml of the cell culture medium was removed and treated with 1 ml of dichloromethane by rotating for 5 min. The supernatant layer was decanted, the organic layer transferred to an HPLC sample tube, and a 20 ml aliquot in-

jected into the C18 reverse-phase HPLC column (Nova-Pak, Waters Corporation, Milford, MA) for chromatographic separation. The mobile phase consisted of 90% methanol-water (50:50; v/v) and 10% glacial acetic acid. A Finnegan LCQ Deca ion trap MS connected to the HPLC column was used to analyze mass distribution of alleles of rat insulin secreted in response to GLP-1 treatment. Insulin was ionized using electro-spray ionization and analyzed in normal mass range ( $m/z$  200–2,000) operation mode to recover the multiple charged peptide alleles.

### GC/MS

Mass spectral data were obtained on the HP5973 mass selective detector connected to an HP6890 gas chromatograph. The settings were as follows: GC inlet 230°C, transfer line 280°C, and MS source 230°C MS Quad 150°C. An HP-5 capillary column (30 m length, 250  $\mu$ m diameter, 0.25  $\mu$ m film thickness) was used for glucose, ribose, glutamate, and lactate analysis. A Bpx70 column (25 m length, 220  $\mu$ m diameter, 0.25  $\mu$ m film thickness; SGE Incorporated, Austin, TX) was used for fatty acid and cholesterol analysis with specific temperature programming for each compound studied. The HPLC instrument used for insulin separation was a multiple module Hewlett Packard 1100 series instrument with a thermally controlled column compartment (Palo Alto, CA).

### Data analysis and statistical methods

In vitro cell culture experiments were carried out using three cultures each time for the GLP-1 treatment regimen in both cell lines and were repeated once. MS analyses were carried out by three independent automatic injections of 1  $\mu$ l sample volume by the automatic sampler and accepted only if the standard sample deviation was less than 1% of the normalized peak intensity. Statistical analyses were performed using the parametric unpaired, two-tailed independent sample *t*-test with 99% confidence intervals ( $\mu \pm 2.58\sigma$ ), and  $P < 0.01$  was considered to indicate significant differences in glucose carbon metabolism in PANC-1 and ARIP epithelial pancreatic carcinoma cells treated with an effective dose of GLP-1.

## RESULTS

For the results reported herein, we incubated ARIP and PDX-1-transfected PANC-1 pancreatic epithelial carcinoma cells in the presence of [1,2- $^{13}\text{C}_2$ ]glucose. The cells were treated with an effective dose (10 nM) of GLP-1 for 48 h. The studied GLP-1 dose was selected based on reports that it triggers an effective ligand-specific cAMP response in receptor-transfected COS-7 cells (21) and also effectively induces ARIP and PANC-1/PDX-1 cells to differentiate into insulin-secreting cells (3). Determining the number of  $^{13}\text{C}$ -labeled carbons and their positions in glucose intermediates showed that both cell lines accumulated the tracer intensively for various intermediate synthetic reactions, and allowed accurate estimation of pathway substrate carbon flow distribution and changes in it, in response to GLP-1 treatment.

HPLC with tandem ion trap electro-spray MS revealed two nonallelic peaks of rat insulin secreted by ARIP cells into the medium after GLP-1 treatment (Fig. 2A). The deconvoluted spectrum (here the first chromatographic peak of rat insulin at retention time 7.53 min is shown) indicated chromatographic and mass spectral distribution

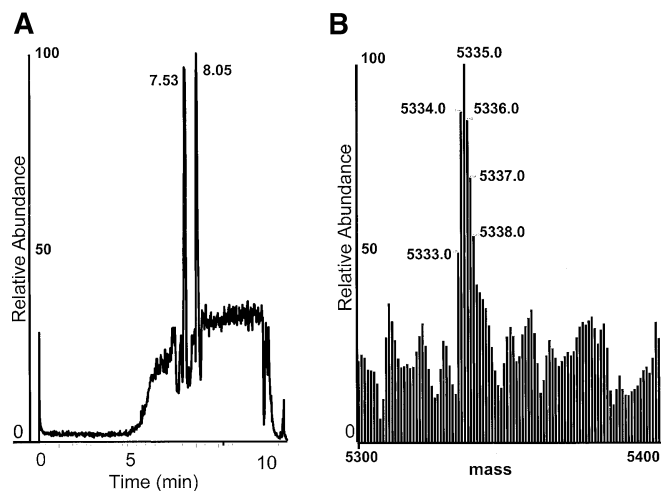


**Fig. 2.** High performance liquid chromatography (HPLC) with tandem ion trap electro-spray mass spectrometry (MS) of insulin in rat pancreatic epithelial (ARIP) cell cultures. HPLC/MS readily reveals the two known nonallelic rat insulin peaks after GLP-1 treatment in ARIP cell cultures (A). The deconvoluted spectra of the peaks (here the one at retention time 7.53 min is shown) (B) reveal mass distribution of rat insulin at 5,333.00 Da.

of rat insulin identical to published data (Fig. 2B) (22). No other peptides were present in detectable levels in the GLP-1-treated ARIP cells' culture media after extended runs in both the positive and negative data collection modes by our LCQ Deca instrument. Control untreated cell culture media did not reveal chromatographic insulin peaks, indicating that no insulin release occurred without GLP-1 treatment in either cell line (not shown).

De novo fatty acid synthesis from glucose is shown in Fig. 3. During the 48 h experimental period, control ARIP and PANC-1 cells synthesized about 22% and 10%, respectively, of their fatty acid (palmitate; C16:0) newly, using carbons obtained from glucose. GLP-1 treatment increased de novo palmitate synthesis significantly in both cell lines and did so markedly in PANC-1 cells, where the de novo synthesis ratio from glucose increased about 8-fold.  $^{13}\text{C}$  incorporation into stearate, the consecutive long-chain saturated fatty acid (C18:0) species, also increased significantly, as shown in Fig. 4. Despite the strong effect on palmitate synthesis and chain elongation,  $^{13}\text{C}$  enrichment of acetyl-CoA (Fig. 5) and de novo cholesterol synthesis (Fig. 6) was not affected by GLP-1 treatment.

The rest of the metabolic profile was uneventful with regard to GLP-1 treatment. Direct glucose oxidation through the pentose cycle with recycling of the pentose yield back into glycolysis were about 2.3% and 3.6% of the glycolytic flux in PANC-1 and ARIP cells, respectively. Pentose cycle activity relative to glycolysis did not show significant changes in either the ARIP or PANC-1 cell cultures after 48 h treatment with 10 nM GLP-1. The amount of lactate in the culture media did not differ significantly among cell lines and treatment groups. Glucose consumption was similar in control and GLP-1-treated cultures of both ARIP and PANC-1 cell lines (Fig. 7A, B).

ARIP cells utilized glucose carbons for nucleic acid syn-



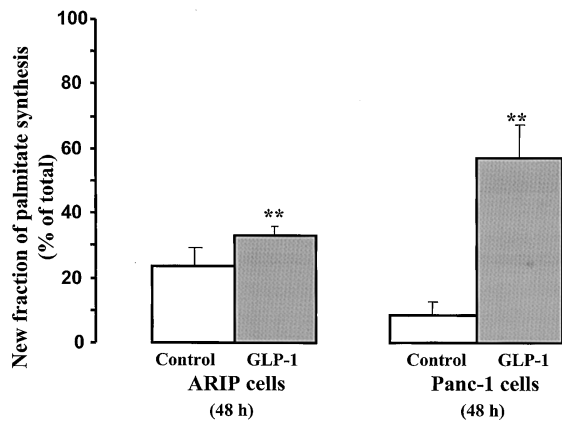


**Fig. 3.** De novo fatty acid (palmitate) synthesis from glucose in cultured ARIP (rat) and ductal tumor (PANC-1) (human) pancreatic epithelial carcinoma cells in the presence of 10 nM GLP-1. ARIP and PANC-1 cells newly synthesize about 22% and 10% of palmitate (C16:0) from the carbons of glucose without treatment (control cultures, empty bars). GLP-1 treatment increases de novo palmitate synthesis significantly in both ARIP and PANC-1 cells after 48 h (dark bars). This increase in palmitate synthesis was rather dramatic in PANC-1 cells, where the de novo synthesis ratio from glucose increased by about 8-fold. (\*\*  $\pm$  SD;  $n = 9$ ).

thesis more intensively than did PANC-1 cells ( $^{13}\text{C } \Sigma m_n$  0.46 vs. 0.37 in ARIP and PANC-1 cells, respectively) and GLP-1 treatment did not alter the accumulation (expressed as total activity,  $\Sigma m_n$ ) of  $^{13}\text{C}$  from glucose into nucleic acid ribose in either cell line (Fig. 7C). The positional accumulation of glucose carbons in nucleic acid ribose through the respective oxidative and nonoxidative reactions of the pentose cycle (expressed as specific activity for each carbon position by the  $\Sigma m/m1$  and  $\Sigma m/m2$  formulas) was also unaffected by GLP-1. It was evident that

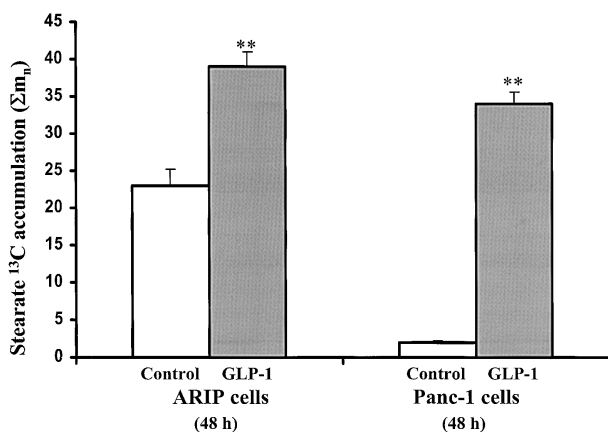


**Fig. 4.** Chain elongation of palmitate into stearate utilizing glucose in cultured ARIP (rat) and PANC-1 (human) pancreatic epithelial carcinoma cells in the presence of 10 nM GLP-1. ARIP and PANC-1 cells elongate about 23% and 2% of stearate (C18:0) utilizing carbons of glucose without treatment (control cultures, empty bars). GLP-1 treatment increases palmitate chain elongation into stearate significantly in both ARIP and PANC-1 cells after 48 h of culturing. This increase in stearate synthesis was rather dramatic in PANC-1 cells, where the de novo synthesis ratio from glucose increased by about 16-fold. (\*\*  $\pm$  SD;  $n = 9$ ).

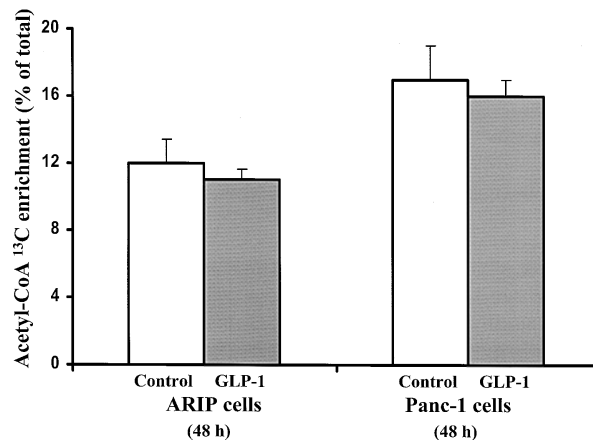


**Fig. 5.** Acetyl-CoA  $^{13}\text{C}$  enrichment from glucose in cultured ARIP (rat) and PANC-1 (human) pancreatic epithelial carcinoma cells in the presence of 10 nM GLP-1. Glucose contributed to about 12% and 17% of acetyl-CoA synthesis in ARIP and PANC-1 cells, as shown by untreated control cultures (empty bars). Ten nanomole GLP-1 treatment did not affect acetyl-CoA  $^{13}\text{C}$  enrichment, indicating the limited role of GLP-1 in modulating the pyruvate dehydrogenase complex of pancreatic cells with epithelial origin during differentiation and insulin synthesis. (Error bars indicate  $\pm$  SD;  $n = 9$ ).

GLP-1 did not affect DNA synthesis rates during the 48 h treatment period because control and treated cells'  $^{13}\text{C } \Sigma m_n$  values were similar in PANC-1 cells and ARIP cells ( $0.111 \pm 0.07$  SD vs.  $0.119 \pm 0.04$  SD) with no apparent changes in response to GLP-1.

TCA cycle anaplerotic flux, which reveals glucose utilization for TCA cycle metabolite synthesis with respect to

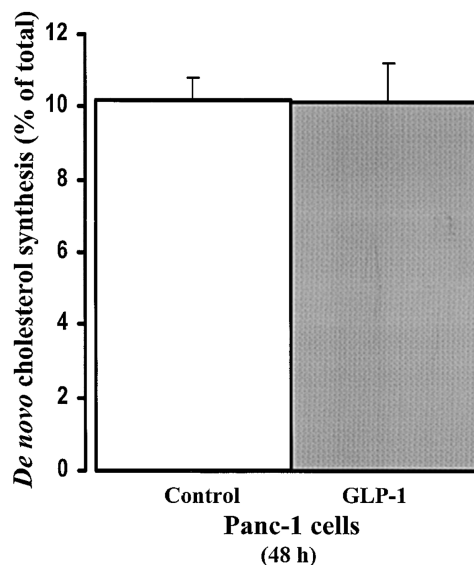


**Fig. 6.** De novo cholesterol synthesis from glucose in cultured PANC-1 (human) pancreatic epithelial carcinoma cells in the presence of 10 nM GLP-1. Glucose contributed to about 10% of de novo cholesterol synthesis in PANC-1 cells, as shown by untreated control cultures (empty bars). Treatment with 10 nM GLP-1 did not affect de novo cholesterol synthesis rates, indicating a limited role of GLP-1 in modulating the cholesterol synthesizing enzymes of pancreatic cells with epithelial origin. (Error bars indicate  $\pm$  SD;  $n = 9$ ).

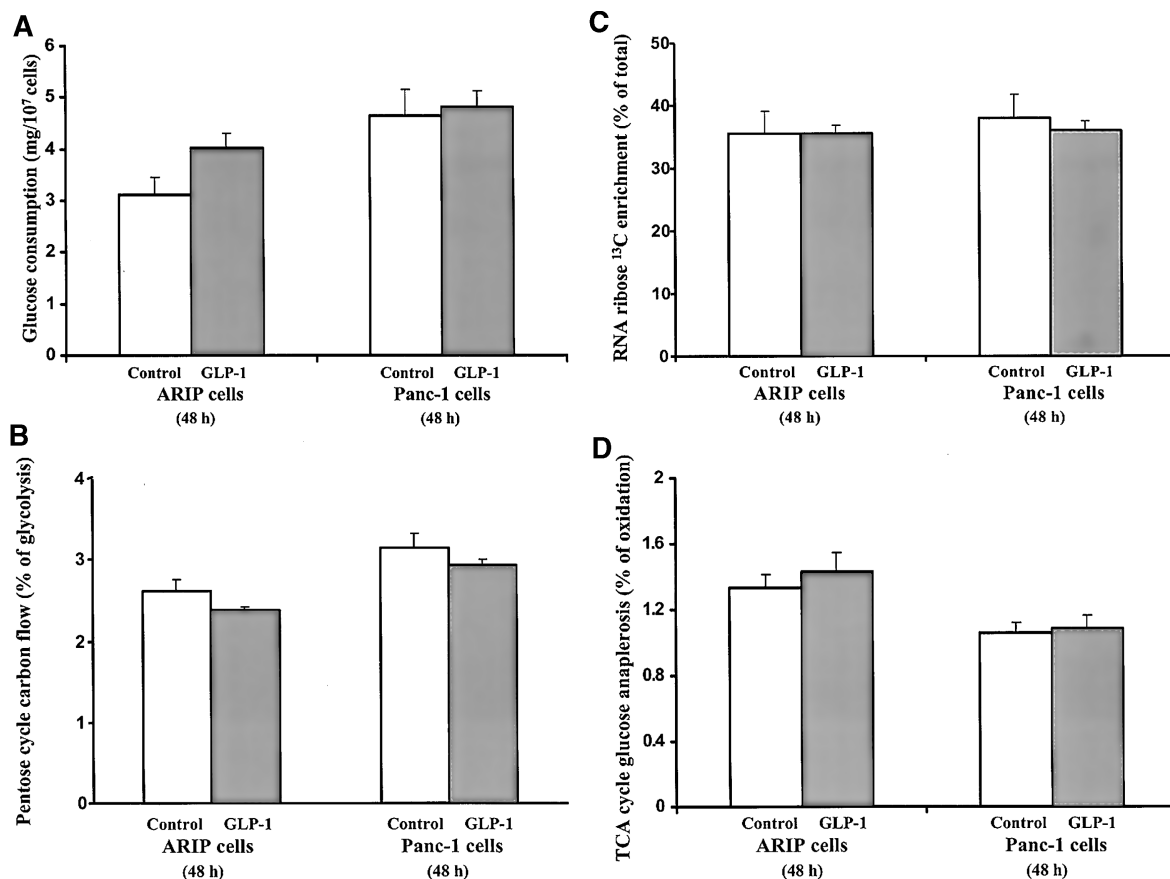


**Fig. 7.** Lack of metabolic effects of 10 nM GLP-1 treatment on glucose consumption, pentose cycle, glycolysis, and TCA cycle carbon flow in ARIP and PANC-1 cells. Glucose consumption was measured by Cobas and corrected for cell number (A). Pentose cycle-direct glucose oxidation and recycling was measured by lactate <sup>13</sup>C labeling patterns (B), nucleic acid ribose synthesis was measured by RNA ribose <sup>13</sup>C accumulation (C), and TCA cycle anaplerosis was measured by glutamate <sup>13</sup>C enrichment (D) as described in the method section. Treatment with 10 nM GLP-1 did not affect any of these metabolic parameters, indicating a limited role of GLP-1 in modulating glucose consumption, pentose cycle carbon flow, and recycling de novo RNA ribose synthesis or TCA cycle glucose oxidation versus anabolic glucose use. (Error bars indicate  $\pm$  SD; n = 9).

glucose oxidation, was measured by glutamate mass isotopomers derived from the tracer. Glutamate stable isotope label rearrangement indicated no significant difference in TCA cycle anaplerotic carbon flux after GLP-1 treatment in the cell lines (Fig. 7D). <sup>13</sup>C-labeled carbon dioxide release from glucose was also unaffected by GLP-1 treatment, which is consistent with the findings noted above, that glucose oxidation in the pentose and TCA cycles is not affected by GLP-1 treatment.

## DISCUSSION

GLP-1 has shown promising effects as a new treatment modality for patients with Type 2 diabetes, but it has a very limited half-life in plasma, so new analogs of this hormone, such as NN2211 (a fatty acid derivative), are currently in clinical trials to determine their safety, tolerability, pharmacokinetics, and pharmacodynamics (23). The results of these clinical trials are controversial; hence additional biochemical and physiological data are necessary to reveal cellular metabolic actions of GLP-1 and its analogs for bet-

ter understanding of their applicability and effectiveness in Type 2 diabetes.

It is known that GLP-1 enhances insulin biosynthesis and secretion as well as transcription of the insulin, GLUT2, and glucokinase genes (26, 27). It has remained, however, a challenge to explain why GLP-1 metabolically affects only de novo fatty acid synthesis and how this phenomenon contributes to the regulation of insulin production, storage, and release.

Data presented here reveal that GLP-1 is a potent agent for the induction of insulin secretion in epithelial cells of the pancreas, and that its mechanisms for doing so through affecting metabolism impact a very narrow range of metabolic targets, only increasing de novo fatty acid palmitate synthesis from glucose and palmitate's chain elongation into stearate.

Such significant effects in the context of limited targets indicate that a selective signaling mechanism is the agent responsible for the differentiation-inducing metabolic effects of this hormone. There is a strong likelihood that the effective mechanism is a PPAR-related nuclear signaling mechanism, since peroxisome regulator ligands pri-

ASBMB  
JOURNAL OF LIPID RESEARCH

marily affect fatty acid synthesis, elongation, and oxidation enzymes through specific nuclear actions (24). Consistent with involvement of a PPAR-related nuclear signaling mechanism are our data indicating that GLP-1 exerts minimal or no effects on glucose uptake, glycolysis, lactate production, TCA cycle anaplerotic flux, acetyl-CoA synthesis, cholesterol production, or on nucleic acid precursor synthesis in the pentose cycle, which is primarily modulated by tyrosine kinase cell-signaling mechanisms, as described previously (25).

There are numerous fatty acids involved in stimulus-secretion coupling mechanisms in the  $\beta$ -cell insulin secretory process. At high levels, glucose and fatty acids synergize and cause toxicity in islets, a process that may be instrumental in the pleiotropic defects associated with the metabolic syndromes associated with Type 1 and Type 2 diabetes. For example, alterations in  $\beta$ -cell malonyl-CoA concentrations, PPAR- $\alpha$  and - $\gamma$ , sterol regulatory element binding protein-1c expression, and lipid partitioning have been proposed to elucidate glucose and fatty acid toxicity on  $\beta$ -cells (26). Corollary to these observations, our data support the hypothesis that the more intense synthesis of fatty acids from glucose and increased elongation of fatty acid chains driven by GLP-1 provide more of the specific fats necessary for membrane packaging, transport, and storage of insulin in the Golgi apparatus. Increased de novo fatty acid synthesis is essential for the formation of differentiated cell structures that require rapidly synthesized intact membranes and receptors, as well as transport vesicles. Granules of protein storage and transport contain between 50–62% triglycerides, which are mainly assembled from nonessential saturated and essential polyunsaturated fatty acids (27). It is likely that in ARIP and PANC-1 cells, newly assembled triglycerides from palmitate and stearate are structurally and functionally involved in the rapid synthesis, transport, and storage of insulin in response to GLP-1 treatment, as palmitate and stearate play important roles as structural components of triglycerides. Palmitate and stearate are also the precursors of further synthesis of the unsaturated nonessential fatty acids, such as oleic acid, phospholipids, and arachidonic acid, which all are substantially involved in secretory vesicle formation and insulin release.

GLP-1 activates protein kinase A and, as such, has been shown to activate hormone-sensitive lipase and induce lipolysis from intracellular triglyceride stores in pancreatic  $\beta$  cells (28). It remains a question as to what extent this effect might influence the results of our experiments. Previous metabolic profiling studies using stable isotope tracers demonstrated that transformed cells depend on de novo fatty acid synthesis (palmitate), chain elongation (stearate), and desaturation (oleate) rather than on triglyceride uptake, storage, and utilization (29). For this reason, we propose that differentiating transformed cells in response to GLP-1 treatment do not primarily utilize lipolysis from intracellular triglyceride pools, as could be expected in normal pancreatic  $\beta$  cells, but also increase de novo fatty acid synthesis, chain elongation, and desaturation as part of their metabolic

adaptation process to GLP-1-induced differentiation and insulin release.

In conclusion, the unique role of GLP-1 in inducing increased glucose carbon substrate flow toward de novo fatty acid synthesis is an important part of the complex regulatory mechanisms through which GLP-1 regulates cell differentiation, insulin synthesis, packaging, and release in mammalian  $\beta$ -cells. SIDMAP, as demonstrated herein, is an important new tool to effectively investigate and understand the mechanisms involved in cell differentiation and insulin secretion processes. Our carbon flow metabolic study data demonstrate the primary effect of GLP-1 on fatty acid synthesis and elongation, and indicate a high likelihood that a nuclear PPAR-related signaling mechanism of this hormone is involved in the regulation of the metabolism of pancreatic cells of epithelial origin. **FIG**

This work was supported by a grant from the Clinical Nutrition and Research Unit of California, its Stable Isotope Core, the National Institutes of Health of the United States, the American Federation for Aging Research, and the Foundation for Diabetes Research.

## REFERENCES

1. Dachicourt, N., P. Serradas, D. Bailbe, M. Kergoat, L. Doare, and B. Portha. 1997. Glucagon-like peptide-1(7–36)-amide confers glucose sensitivity to previously glucose-incompetent beta-cells in diabetic rats: *in vivo* and *in vitro* studies. *J. Endocrinol.* **155**: 369–376.
2. Montrose-Rafizadeh, C., Y. Wang, A. M. Janczewski, T. E. Henderson, and J. M. Egan. 1997. Overexpression of glucagon-like peptide-1 receptor in an insulin-secreting cell line enhances glucose responsiveness. *Mol. Cell. Endocrinol.* **130**: 109–117.
3. Hui, H., C. Wright, and R. Perfetti. 2001. Glucagon-like peptide 1 induces differentiation of islet duodenal homeobox-1-positive pancreatic ductal cells into insulin-secreting cells. *Diabetes.* **50**: 785–796.
4. Zhou, J., C. Montrose-Rafizadeh, A. M. Janczewski, M. A. Pineyro, S. J. Sollott, Y. Wang, and J. M. Egan. 1999. Glucagon-like peptide-1 does not mediate amylase release from AR42J cells. *J. Cell. Physiol.* **181**: 470–478.
5. Salapatek, A. M., P. E. MacDonald, H. Y. Gaisano, and M. B. Wheeler. 1999. Mutations to the third cytoplasmic domain of the glucagon-like peptide 1 (GLP-1) receptor can functionally uncouple GLP-1-stimulated insulin secretion in HIT-T15 cells. *Mol. Endocrinol.* **13**: 1305–1317.
6. Wang, X., J. Zhou, M. E. Doyle, and J. M. Egan. 2001. Glucagon-like peptide-1 causes pancreatic duodenal homeobox-1 protein translocation from the cytoplasm to the nucleus of pancreatic beta-cells by a cyclic adenosine monophosphate/protein kinase A-dependent mechanism. *Endocrinology.* **142**: 1820–1827.
7. Hussain, M. A., and J. F. Habaner. 2000. Glucagon-like peptide-1 increases glucose-dependent activity of the homeoprotein PDX-1 transactivating domain in pancreatic beta cells. *Biochem. Biophys. Res. Commun.* **274**: 616–619.
8. Cascante, M., L. G. Boros, B. Comin-Anduix, P. de Atauri, J. J. Centelles, and P. W. Lee. 2002. Metabolic control analysis in drug discovery and disease. *Nat. Biotechnol.* **20**: 243–249.
9. Boros, L. G., M. Cascante, and W. N. Paul Lee. 2002. Metabolic profiling of cell growth and death in cancer: applications in drug discovery. *Drug Discov. Today.* **7**: 364–372.
10. Boros, L. G., J. S. Torday, S. Lim, S. Bassilian, M. Cascante, and W. N. Lee. 2000. Transforming growth factor beta2 promotes glucose carbon incorporation into nucleic acid ribose through the nonoxidative pentose cycle in lung epithelial carcinoma cells. *Cancer Res.* **60**: 1183–1185.
11. Boren, J., M. Cascante, S. Marin, B. Comin-Anduix, J. J. Centelles,

- S. Lim, S. Bassilian, S. Ahmed, W. N. Lee, and L. G. Boros. 2001. Gleevec (STI571) influences metabolic enzyme activities and glucose carbon flow toward nucleic acid and fatty acid synthesis in myeloid tumor cells. *J. Biol. Chem.* **276**: 37747–37753.
12. Boros, L. G., K. Lapis, B. Szende, R. Tomoskozi-Farkas, A. Balogh, J. Boren, S. Marin, M. Cascante, and M. Hidvegi. 2001. Wheat germ extract decreases glucose uptake and RNA ribose formation but increases fatty acid synthesis in MIA pancreatic adenocarcinoma cells. *Pancreas*. **23**: 141–147.
  13. Comin-Anduix, B., L. G. Boros, S. Marin, J. Boren, C. Callol-Masot, J. J. Centelles, J. L. Torres, N. Agell, S. Bassilian, and M. Cascante. 2002. Fermented wheat germ extract inhibits glycolysis/pentose cycle enzymes and induces apoptosis through poly(ADP-ribose) polymerase activation in Jurkat T-cell leukemia tumor cells. *J. Biol. Chem.* **277**: 46408–46414.
  14. Kasho, K., S. Cheng, D. M. Jensen, H. Ajje, W. N. Lee, and L. D. Faller. 1996. Feasibility of analyzing [<sup>13</sup>C]urea breath tests for *Helicobacter pylori* by gas chromatography-mass spectrometry in the selected ion monitoring mode. *Aliment. Pharmacol. Ther.* **10**: 985–995.
  15. Neese, R. A., S. Q. Siler, D. Cesar, F. Antelo, D. Lee, L. Misell, K. Patel, S. Tehrani, P. Shah, and M. K. Hellerstein. 2001. Advances in the stable isotope-mass spectrometric measurement of DNA synthesis and cell proliferation. *Anal. Biochem.* **298**: 189–195.
  16. Lee, W. N., L. G. Boros, J. Puigianer, S. Bassilian, S. Lim, and M. Cascante. 1998. Mass isotopomer study of the non-oxidative pathways of the pentose cycle with [1,2-<sup>13</sup>C<sub>2</sub>]glucose. *Am. J. Physiol.* **274**: E843–E851.
  17. Lee, W. N., J. Edmond, S. Bassilian, and J. W. Morrow. 1996. Mass isotopomer study of glutamine oxidation and synthesis in primary culture of astrocytes. *Dev. Neurosci.* **18**: 469–477.
  18. Leimer, K. R., R. H. Rice, and C. W. Gehrke. 1977. Complete mass spectra of N-TAB esters of amino acids. *J. Chromatogr.* **141**: 121–144.
  19. Lee, W. N. 1996. Stable isotopes and mass isotopomer study of fatty acid and cholesterol synthesis. A review of the MIDA approach. *Adv. Exp. Med. Biol.* **399**: 95–114.
  20. Khaksa, G., K. Nalini, M. Bhat, and N. Udupa. 1998. High-performance liquid chromatographic determination of insulin in rat and human plasma. *Anal. Biochem.* **260**: 92–95.
  21. Takhar, S., S. Gyomory, R. C. Su, S. K. Mathi, X. Li, and M. B. Wheeler. 1996. The third cytoplasmic domain of the GLP-1[7–36 amide] receptor is required for coupling to the adenylyl cyclase system. *Endocrinology*. **137**: 2175–2178.
  22. Gishizky, M. L., and G. M. Grodsky. 1987. Differential kinetics of rat insulin I and II processing in rat islets of Langerhans. *FEBS Lett.* **223**: 227–231.
  23. Agero, H., L. B. Jensen, B. Elbrond, P. Rolan, and M. Zdravkovic. 2002. The pharmacokinetics, pharmacodynamics, safety and tolerability of NN2211, a new long-acting GLP-1 derivative, in healthy men. *Diabetologia*. **45**: 195–202.
  24. Schoonjans, K., B. Staels, and J. Auwerx. 1996. The peroxisome proliferator activated receptors (PPARs) and their effects on lipid metabolism and adipocyte differentiation. *Biochim. Biophys. Acta*. **1302**: 93–109.
  25. Gong, T. W., D. J. Meyer, J. Liao, C. L. Hodge, G. S. Campbell, X. Wang, N. Billestrup, C. Carter-Su, and J. Schwartz. 1998. Regulation of glucose transport and c-fos and egr-1 expression in cells with mutated or endogenous growth hormone receptors. *Endocrinology*. **139**: 1863–1871.
  26. Prentki, M., E. Joly, W. El-Assaad, and R. Roduit. 2002. Malonyl-CoA signaling, lipid partitioning, and glucolipotoxicity: role in beta-cell adaptation and failure in the etiology of diabetes. *Diabetes*. **51(Suppl 3)**: S405–S413.
  27. Zhou, Y. T., M. Shimabukuro, Y. Lee, K. Koyama, M. Higa, T. Ferguson, and R. H. Unger. 1998. Enhanced *de novo* lipogenesis in the leptin-unresponsive pancreatic islets of prediabetic Zucker diabetic fatty rats: role in the pathogenesis of lipotoxic diabetes. *Diabetes*. **47**: 1904–1908.
  28. Hashiguchi, S., T. Yada, and T. Arima. 2001. A new hypoglycemic agent, JTT-608, evokes protein kinase A-mediated Ca(2+) signaling in rat islet beta-cells: strict regulation by glucose, link to insulin release, and cooperation with glucagon-like peptide-1 (7–36)amide and pituitary adenylate cyclase-activating polypeptide. *J. Pharmacol. Exp. Ther.* **296**: 22–30.
  29. Lee, W. N., S. Lim, S. Bassilian, E. A. Bergner, and J. Edmond. 1998. Fatty acid cycling in human hepatoma cells and the effects of troglitazone. *J. Biol. Chem.* **273**: 20929–20934.